 ICCES, vol.3, no.1, pp.1-7, 2007

Phase Field Simulations Of Stress-Free Ferroelectric Nanoparticles With Different Long-Range Electrostatic Interactions

Jie Wang[1] and Tong-Yi Zhang[1]

Summary

Two-dimensional phase field simulations of stress-free ferroelectric nanoparticles with different long-range (LR) electrostatic interactions are conducted based on the time-dependent Ginzburg-Landau equation. Polarization patterns and the toroidal moment of polarization are found to be dependent on the LR electrostatic interaction and the size of the simulated nanoparticle. Phase field simulations exhibit vortex patterns with purely toroidal moments of polarization and negligible macroscopic polarization in the stress-free ferroelectric nanoparticles when the LR electrostatic interaction is fully taken into account. However, a single-domain structure without any toroidal moment of polarization is formed in small particles if the LR electrostatic interaction is completed ignored. The result indicates that the LR electrostatic interaction and the particle size play crucial roles in the formation of polarization vortices in the ferroelectric nanoparticles.

Introduction

Ferroelectric properties in low dimensional structures, such as, the ferroelectric epitaxial islands[1−4] and thin films[5−8], ferroelectric nanotubes and nanorods[9,10] and ferroelectric particles[11,12] have been investigated with a great deal of interest due to the potential integration of nanoscale ferroelectrics into microelectronics. Due to the LR electrostatic interaction, the 180^o stripe domains are energetically favorable[7] in ferroelectric thin films. The LR electrostatic interaction is also able to quench spontaneous polarization.[13,14] The formation of polarization patterns in low dimensional ferroelectric structures depends also strongly on the LR elastic interaction induced by spontaneous strains.[14] To reduce elastic interaction energy, 90^o multidomains are energetically favorable in constrained ferroelectrics.[15] Thus, the polarization patterns in ferroelectric particles are much complex[16], due to the competition between the LR elastic and electrostatic interactions, and other kinds of energies.

Previous studies [1−16] about low dimensional ferroelectric structures mainly focused on the size-dependent polarization and other material properties averaged over an interested dimension(s). Recently, the toroid moment **G** of polarization was found in ferroelectric nanodisks and nanorods from *ab initio* simulations.[17] The toroid moment, characterized for a clockwise or anti-clockwise vortice, is bistable.

[1]Corresponding author, Tel: (852) 2358-7192, Fax: (852) 2358-1543, E-mail: mezhangt@ust.hk. Department of Mechanical Engineering, Hong Kong University of Science and Technology, Clear Water Bay, Kowloon, Hong Kong, China

The toroidal moment can be switched from one stable state to the other by applying a time-dependent magnetic field. Storing data using a switchable macroscopic toroidal moment could be superior to using the macroscopic polarization[17], because generating a magnetic field—unlike the generation of electric field—does not require electrode contact. Fabricating electrode contact could be a challenging issue in manufacturing nanoscale devices.

Based on the time-dependent Ginzburg-Landau equation, we simulate, in the present work, the effects of the particle size and the LR electrostatic interaction on the toroidal moment of polarization in two-dimensional stress-free ferroelectric nanoparticles. The LR electrostatic interactions are controlled by a weight parameter, β, which is assigned to the electrostatic energy in the simulations. We study two cases (i) $\beta = 1$ corresponds to the ideal open-circuit electrical boundary condition, in which the electrostatic interactions are fully taken into account without any screening; and (ii) $\beta = 0$ corresponds to the ideal short-circuit electrical boundary condition, in which the electrostatic interactions are completely screened.

Simulation Methodology

In ferroelectric phase-field simulations[14−16,18−22], it is usually assumed that the mechanical and electrical equilibrium is established instantaneously for a given distribution of spontaneous polarization even that applied mechanical and electric fields change the distribution of spontaneous polarization. Thus, the spontaneous polarization **P**=(P_1, P_2, P_3) is taken as the order parameter and the temporal evolution of the domain structure is calculated from the time-dependent Ginzburg-Landau equation,

$$\frac{\partial P_i(\mathbf{r},t)}{\partial t} = -L\frac{\delta F}{\delta P_i(\mathbf{r},t)} \quad (i = 1,2,3), \tag{1}$$

where L is the kinetic coefficient, $\mathbf{r}$ and t denote the spatial vector and time, respectively, and F is the total fee energy. The total free energy of stress-free ferroelectrics can be expressed as

$$F = \int_V (f_{LD}(P_i) + f_G(P_{i,j}) + \beta f_{Dep}(E_i^d, P_i))dV, \tag{2}$$

in which f_{LD} is the Landau free energy density, which can be expressed by[23]

$$\begin{aligned} f_{LD}(P_i) =& \alpha_1(P_1^2+P_2^2+P_3^2) + \alpha_{11}(P_1^4+P_2^4+P_3^4) + \alpha_{12}(P_1^2P_2^2+P_2^2P_3^2+P_1^2P_3^2) \\ &+ \alpha_{111}(P_1^6+P_2^6+P_3^6) + \alpha_{112}[(P_1^4(P_2^2+P_3^2)+P_2^4(P_1^2+P_3^2)+P_3^4(P_1^2+P_2^2)] \\ &+ \alpha_{123}P_1^2P_2^2P_3^2, \end{aligned} \tag{3}$$

where $\alpha_1 = (T-T_0)/2\varepsilon_0 C_0$ is the dielectric stiffness, α_{11}, $\alpha_{12}\alpha_{111}\alpha_{112}$, α_{123} are higher order dielectric stiffnesses, T and T_0 denote temperature and the Curie-Weiss

temperature, respectively, C_0 is the Curie constant. The term of $f_G(P_{i,j})$ in Eq.(2) is gradient energy density[15,16] , which has the form as

$$\begin{aligned} f_G(P_{i,j}) =& \frac{1}{2}G_{11}(P_{1,1}^2 + P_{2,2}^2 + P_{3,3}^2) + G_{12}(P_{1,1}P_{2,2} + P_{2,2}P_{3,3} + P_{1,1}P_{3,3}) \\ &+ \frac{1}{2}G_{44}[(P_{1,2} + P_{2,1})^2 + (P_{2,3} + P_{3,2})^2 + (P_{1,3} + P_{3,1})^2] \\ &+ \frac{1}{2}G_{44}^{'}[(P_{1,2} - P_{2,1})^2 + (P_{2,3} - P_{3,2})^2 + (P_{1,3} - P_{3,1})^2], \end{aligned} \tag{4}$$

where G_{11}, G_{12}, G_{44}, and $G_{44}^{'}$ are gradient energy coefficients, and $P_{i,j}$ denotes the derivative of the ith component of the polarization vector, P_i, with respect to the jth coordinate and i,j =1, 2, 3. The last term, f_{Dep}, in Eq. (2) is the LR electrostatic interaction energy density, which is described by[24]

$$f_{Dep} = -\frac{1}{2}(E_1^d P_1 + E_2^d P_2 + E_3^d P_3), \tag{5}$$

where E_1^d, E_2^d and E_3^d are the three components of electrostatic field vector along the x_1, x_2 and x_3 axes, respectively. In the present study, the method used in Ref.[14] is adopted here to calculate the electrostatic field, excepting that the weight of β is assigned to the electrostatic energy term in Eq.(2) to control the magnitude of the LR electrostatic interaction. The finite difference method for spatial derivatives and the Runge-Kutta method of order four for temporal derivatives are employed to solve Eq. (1) in real space with the boundary condition of $dP_i/dn = -P_i/\delta$, in which n refers unit length in the normal direction of the surface and δ is the extrapolation length.

Dimensionless variables[15] are used in the present simulations. The material constants adopted in the present simulations are the same as those used in Ref [14], except that a dimensionless factor, β, zero or one, is assigned to the LR electrostatic interaction energy. The value of the extrapolation length, δ, is 3 in the present study.[12] We use 20×20 discrete grids to represent a 2D square particle and each grid has a dimensionless area of $a \times a$. The grid size, a, is assigned different values to represent different sizes of ferroelectrics. The polarization varies spatially and is characterized at each grid by a two-component vector, or an electric dipole, of which the length and direction denote the magnitude and direction of the dipole, respectively. The time step is set to $\Delta t = 0.004$ and the total number of steps in solving Eq. (1) is 8000, which is sufficient for the simulated system to reach a steady state[15]. In the present study, we report simulation results only at the steady state at room temperature.

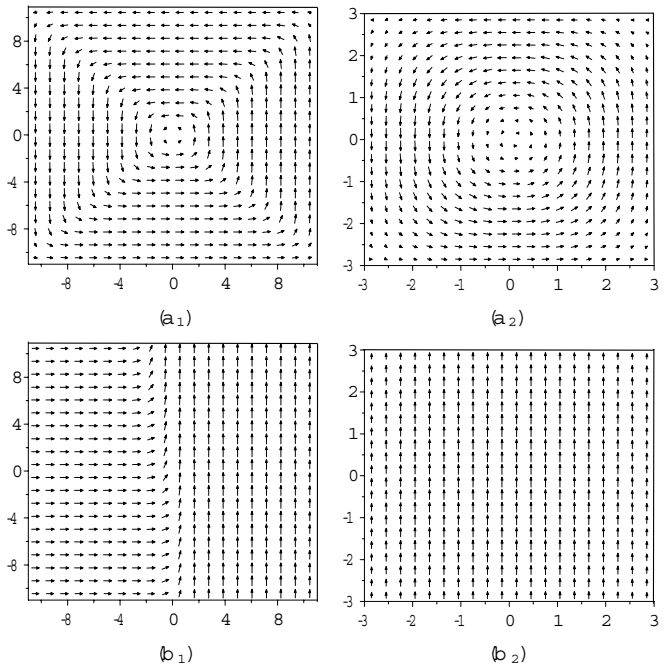

Figure 1: Size dependence of polarization patterns in stress-free 2D ferroelectrics with $\beta = 1$ in (a_1)-(a_2) and $\beta = 0$ in (b_1)-(b_2).

Simulation Results

Figs.1 (a_1)-(a_2) and (b_1)-(b_2) show the polarization patterns of the stress-free 2D square ferroelectrics with $\beta = 1$ and 0, respectively, where Figs. 1(a_1) and (b_1) and Figs. 1(a_2) and (b_2) are for the simulated dimensionless sizes of 22 and 6, respectively, with one unit in the dimensionless size corresponding to 1 nm in the real size[16]. The case of $\beta = 1$ corresponds to the ideal open-circuit electrical boundary condition, in which the electrostatic interactions are fully taken into account. Under the ideal open-circuit electrical boundary condition, the polarizations form a vortex pattern, as shown in Figs. 1(a_1) and (a_2), and the macroscopic polarization, defined as $< \mathbf{P} >= (N)^{-1} \sum_k \mathbf{P}_k$,[17] is found to be zero, i.e., $< \mathbf{P} >= 0$, where N is the number of cells in the simulation. The vortex pattern may also be regarded as having a domain structure with four domains and four wide 90° domain walls, which is caused by the square shape of the simulated ferroelectrics. When the particle size is reduced from 22 to 6, the 90° domain structure becomes obscure and the vortex pattern is more distinct. The case of β=0 corresponds to ideal short-circuit electrical boundary condition, in which the electrostatic interactions are completely screened. When the particle size is 22, the polarizations form two domains with a 90° domain wall. The wall is almost perpendicular to the polar-

izations in one domain and parallel to the polarizations in the other domain. This kind of a 90^o domain wall is different from the normal 90° domain wall induced by the LR elastic interaction, in which the wall has an angle of 45^o with polarizations in both domains. The two domain structure shown in Fig. (b1) is formed by the reduction in the Landau free energy. With the size decreasing, the gradient energy becomes predominate in comparison with the Landau free energy, therefore, the polarization pattern changes from the multidomain state to a monodomain state. Fig.1 (b2) shows the monodomain structure with a dimensionless particle size of 6. The formation of single domain is to reduce the gradient energy. Nevertheless, no vortex exhibits due to the absence of the LR electrostatic interaction for both sizes, as shown in Figs. (b1) and (b2).

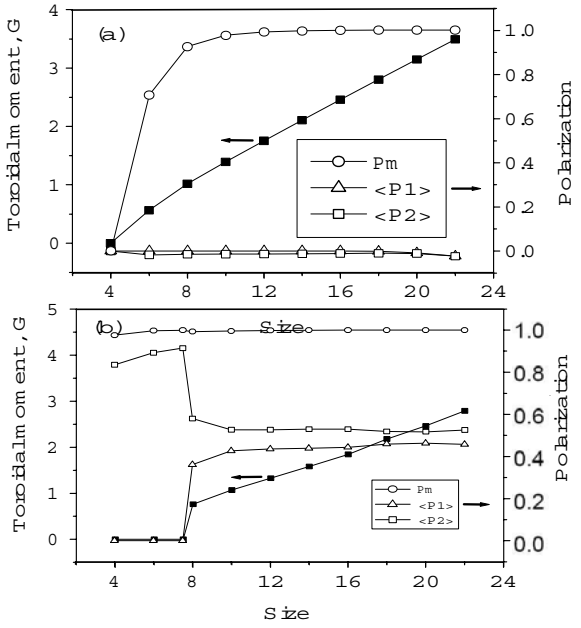

Figure 2: The polarization moment, **G**, on the left vertical axis, and the total macroscopic polarization components, $< P_1 >$ and $< P_2 >$, and the magnitude of the maximum polarization, P_m, on the right vertical axis, as functions of the simulated ferroelectrics size with $\beta = 1$ in (a) and $\beta = 0$ in (b).

Figs. 2(a) and 2(b) illustrate the toroidal moment of polarization, **G**, the total macroscopic polarization components, $< P_1 >$ and $< P_2 >$, and the magnitude of the maximum polarization, $P_m = \max\{|\mathbf{P}_k|\}$ as a function of the particle size for β = 1 and 0, respectively. The toroidal moment of polarization, **G**, is defined as $G = (2N)^{-1}\sum_i R_i \times p_i$, where p_i is the local dipole of cell i located at R_i. When $\beta = 1$, both the moment and the magnitude of the maximum polarization decrease

with the decreases of the particle size and become zero at the size of 4, as shown in Fig.2 (a). With $\beta = 1$, the polarizations form a vortex for all simulated sizes and the total macroscopic polarization components, $< P_1 >$ and $< P_2 >$, are almost equal to zero, thereby indicating that the vortex pattern does not exhibit any macroscopic polarization. The vortex pattern without any macroscopic polarization is very important for memory nanodevices[17]. The null macroscopic polarization does not produce a strong electric field that has a LR character. The vortex structure with nonzero toroidal moment of polarization in a single nanoparticle can therefore be switched without disturbing the states of its neighboring particles. Consequently, the toroidal moment carriers, i.e., the nanoparticles, can thus be packed considerably more densely than the conventional carriers of macroscopic polarizations, giving rise to a marked improvement in the density of ferroelectric recording. In the case of $\beta = 0$, the polarization pattern changes from the multidomain state to the monodomain state as the size is reduced to 8, which results in the abrupt disappearance of the toroidal moment of polarization, as shown in Fig. 2(b). The total net polarizations, P_m and $< P_2 >$, are both nonzero, as shown in Fig. 2(b). Furthermore, the magnitude of the maximum polarization still maintains a high value even at the size of 4, at which the polarizations are both zeros in the case of $\beta = 1$, as shown in Fig. 2(a).

Conclusions

In summary, the two-dimensional simulations demonstrate that the LR electrostatic interaction has a significant influence on the formation of polarization vortex with purely toroidal moments and negligible macroscopic polarization in stress-free ferroelectric nanoparticles. The simulations exhibit vortex patterns with purely toroidal moments of polarization and negligible macroscopic polarizations when the LR electrostatic interactions are fully taken into account. However, a single-domain structure without any toroidal moment of polarization is formed when the LR electrostatic interaction is completely screened and when the particle size is smaller than 8 nm.

Acknowledgement

This work was fully supported by a RGC grant from the Research Grants Council of the Hong Kong Special Administrative Region, China.

References

1. K. Lee, K. Kim, S.J. Kwon, and S. Baik, Appl. Phys. Lett. **85**, 4711 (2004).
2. M. W. Chu, I. Szafraniak, R. Scholz, C. Harnagea, D. Hesse, M. Alexe and U. Gosele, Nature

   Materials **3**, 87 (2004)
3. V. Nagarajan, S. Prasertchoung, T. Zhao, H. Zheng, J. Ouyang, R. Rameshb,

W. Tian, X. Q. Pan, D. M. Kim, C. B. Eom, H. Kohlstedt and R. Waser, Appl. Phys. Lett., **84**, 5225 (2004)

4. A. Roelofs, T. Schneller, K. Szot and R. Waser, Appl. Phys. Lett. **81**, 5231 (2002).
5. J. Junquera, and P. Ghosez, Nature **422**, 506 (2003)
6. T.M. Shaw, S. Trolier-McKinstry, and P.C. McIntyre, Annu. Rev. Mater. Sci. **30**, 263 (2000).
7. D. D. Fong, G.B. Stephenson, S.K. Streiffer, J.A. Eastman, O. Auciello, P.H. Fuoss, and C. Thompson, Science **304**, 1650 (2004).
8. C. H. Ahn, K. M. Rabe, and J.-M. Triscone, Science **303**, 488 (2004).
9. Y. Luo, I. Szafraniak, V. Nagarajan, R.B. Wehrspohn, M. Steinhart, J.H. Wendorff, N.D. Zakharov, R. Ramesh, and M. Alexe, Integrated Ferroelectrics **59**, 1513 (2003).
10. G. Suyal, E. Colla, R. Gysel, M. Cantoni, and N. Setter, Nano Lett. **4**, 1339 (2004).
11. B. Jiang, J. L. Peng, L. A. Bursill, and W. L. Zhong, J. Appl. Phys. **87**, 3462 (2000).
12. W.L. Zhong, Y.G. Wang, P.L. Zhang, and B.D. Qu, Phys. Rev. B **50**, 698 (1994).
13. W. S.Yun, J. J. Urban, Q. Gu, and H. Park, Nano Lett. **2**, 447 (2002).
14. J. Wang, and T.Y. Zhang, Appl. Phys. Lett., **88**, 182904 (2006).
15. J. Wang, S.Q. Shi, L.Q. Chen, Y.L. Li, and T.Y. Zhang, Acta. mater. **52**,749 (2004).
16. Y.L. Li, S.Y. Hu, Z.K. Liu, and L.Q. Chen, Acta. Mater. **50**, 395 (2002).
17. I. I. Naumov, L. Bellaiche, and H. Fu, Nature **432**, 737 (2004).
18. S. Nambu, and D.A. Sagala, Phys. Rev. B **50**, 5838 (1994).
19. H.L. Hu, and L.Q. Chen, Mater. Sci. Eng. A **238**,182 (1997).
20. R. Ahluwalia, and W. Cao, J. Appl. Phys. **93**, 537 (2003).
21. W. Cao, S. Tavener, and S. Xie, J. Appl. Phys. **86**, 5739 (1999).
22. Y.L. Li, S.Y. Hu, Z.K. Liu, and L.Q. Chen, Appl. Phys. Lett. **81**, 427 (2002).
23. M.J. Haun, E. Furman, S.J. Jang, H.A. McKinstry, and L.E. Closs, J. Appl. Phys. **62**, 3331 (1987).
24. M.E. Lines, and A.M. Glass, Principles and applications of ferroelectrics and related materials, (Clarendon press, Oxford, 1977).